

Parametric perspective on highly excited states: case studies of CHBrClF and C₂H₂

Aravindan Semparithi and Srihari Keshavamurthy

Department of Chemistry, Indian Institute of Technology, Kanpur, India 208 016

Considerable insights can be obtained regarding the nature of highly excited states by computing the eigenbasis expectation values of the resonance operators associated with an effective spectroscopic Hamiltonian. The expectation values are related to the parametric derivative of the eigenvalues with respect to specific resonance strengths *i.e.*, level velocities. Sensitivity of the level velocities to the existence of closed orbits in the underlying classical phase space provides for a dimensionality independent route to a dynamical assignment of the states. In this letter, taking CHBrClF (polyad $P = 5$) and the $[16, 0]^{g+}$ bend polyad of C₂H₂ as examples, we show that the level velocities can signal the birth of new modes and highlight sequences of localized eigenstates.

I. INTRODUCTION

Dynamical assignment of the highly excited eigenstates of a polyatomic molecule is a topic of significant interest to the chemical physics community[1, 2, 3, 4]. Insights into the nature of the excited states provides for a better understanding of the phenomenon of intramolecular vibrational energy redistribution (IVR) occurring in the molecule[1, 3, 4]. Assignment of the low energy vibrational states in terms of the usual normal mode quantum numbers is relatively straightforward. However with increasing energies the normal mode quantum numbers are no longer conserved due to perturbations that strongly mix the zeroth order modes and the molecular vibrational Hamiltonian[4] takes the form:

$$\begin{aligned} \hat{H} &= \sum_{i=1}^N \nu_i \hat{v}_i + \sum_{i<j=1}^N x_{ij} \hat{v}_i \hat{v}_j + \dots + \sum_k \tau_k \hat{V}_k(\hat{\mathbf{a}}_k, \hat{\mathbf{a}}_k^\dagger) \\ &\equiv \hat{H}_0(\hat{\mathbf{v}}) + \sum_k \tau_k \hat{V}_k(\hat{\mathbf{a}}_k, \hat{\mathbf{a}}_k^\dagger) \end{aligned} \quad (1)$$

wherein H_0 represents the Dunham expansion, x_{ij} are the anharmonic constants and \hat{V}_k are the various perturbations. The operators \hat{a}_k and \hat{a}_k^\dagger represent the annihilation and creation operators for the k^{th} mode respectively. The normal mode quantum numbers $v_i = \hat{a}_i^\dagger \hat{a}_i$, sufficient for assigning low energy eigenstates, do not commute with \hat{V}_k and hence cannot be used to assign the eigenstates of \hat{H} . The above Hamiltonian is usually generated from a fit to the experimental spectrum in the absence of a global *ab initio* potential energy surface. Even in the case when an accurate potential energy surface is at hand it is possible, and useful, to generate a Hamiltonian of the above form using the canonical Van-Vleck perturbation theory[5, 6]. The advantages of using Hamiltonians of the above form stems from the fact that the classical limit Hamiltonian

$$H(\mathbf{I}, \boldsymbol{\theta}) = H_0(\mathbf{I}) + 2 \sum_k \tau_k f_k(\mathbf{I}) \cos(\mathbf{m}_k \cdot \boldsymbol{\theta}) \quad (2)$$

is easily obtained via the correspondence $\hat{\mathbf{a}} \leftrightarrow \sqrt{\mathbf{I}}e^{-i\boldsymbol{\theta}}$. The f -dimensional vector \mathbf{m}_k has integer components (r_1, r_2, \dots, r_f) and $(\mathbf{I}, \boldsymbol{\theta})$ are the action-angle variables[7]

corresponding to H_0 . The order of a resonance[7] is defined as $O_k \equiv \sum_{j=1}^f |r_j|$. The perturbations $V_k(\mathbf{I}, \boldsymbol{\theta}) \equiv f_k(\mathbf{I}) \cos(\mathbf{m}_k \cdot \boldsymbol{\theta})$ are called resonant because the condition $\mathbf{m}_k \cdot \boldsymbol{\Omega}(\mathbf{I}) = 0$ implies a specific commensurability or locking between the unperturbed frequencies $\boldsymbol{\Omega}(\mathbf{I}) \equiv \partial H_0(\mathbf{I})/\partial \mathbf{I}$. Such resonances are responsible for energy flow through the molecule and lead to breakdown of the zeroth order, low energy quantum numbers. Classical dynamics of resonant Hamiltonians is historically very rich and have been studied in great detail[7]. In particular a detailed understanding of the classical dynamics of $H(\mathbf{I}, \boldsymbol{\theta})$ is essential for any dynamical assignment of the quantum eigenstates of \hat{H} . Furthermore the effective Hamiltonian approach utilizes the state space perspective which offers considerable advantages towards understanding IVR[4].

Clearly any assignment of the eigenstates of \hat{H} formally requires the existence of a sufficiently large set of good quantum numbers. Such a set does not exist in general and hence assignment implies the existence of at least approximate or quasi quantum numbers. By necessity such approximate quantum numbers are conserved for a certain time period dictated by the dynamics of the system. Support for the notion of quasi quantum numbers partially comes from the experimental observation[4] of hierarchical IVR in molecules and the fact that most molecules are not ergodic even at fairly high energies[8]. In this sense deciphering the quantum numbers, exact or approximate, invariably implies the knowledge of the underlying dynamics. Consequently one speaks of a dynamical assignment of the eigenstates wherein some or all of the quantum numbers arise by focusing on important quantum and or classical dynamical structures. A consistent picture that is emerging from many studies is that the complicated spectral splittings and patterns at high energies can be ‘unzipped’ to some extent using the underlying classical dynamics. More specifically, *the spectra are unzipped by recognizing eigenstates showing similar localization characteristics about important classical invariant structures in the underlying phase space.*

Studies based on classical-quantum correspondence have been successfully applied to systems with two coupled modes[9, 10, 11, 12, 13, 14, 15, 16] but are yet to be extended to systems with three or more coupled modes

i.e., multimode systems[17]. The technical and conceptual difficulties associated with a straightforward generalization of the two mode techniques to multimode systems are well understood[15]. Circumventing the technical difficulty, in our opinion, requires utilizing quantum objects which are sensitive to the underlying classical mechanics but do not rely on visualizing the phase space and eigenstates. Considerable work has been done in this direction and a common theme underlying such approaches is the analysis of the eigenvalues and their variation with Hamiltonian parameters[18, 19, 20, 21, 22, 23]. For instance the nature of an eigenstate $|\alpha\rangle$ of \hat{H} has been studied using the methods of diabatic correlations[19, 20] revealing the existence of formal quantum numbers. The basic quantity in these studies is the variation of the eigenvalue E_α with a specific coupling strength *i.e.*, $\partial E_\alpha/\partial\tau_k$. Remarkable correlation of the level variations to the phase space nature of the eigenstates had been noted by Weissman and Jortner in the context of the Henon-Heiles system[24]. Support for the correlation was provided recently[25] from a semiclassical viewpoint and it was suggested that the parametric variations were sensitive to the various bifurcations occurring in the classical phase space. However strong support for the observed correlations have existed[26] in the literature in terms of the classical-quantum correspondence of quantum expectation values *i.e.*, diagonal matrix elements.

In order to elucidate the connections we note that the Hellman-Feynman theorem

$$V_k^{\alpha\alpha} \equiv \langle\alpha|\hat{V}_k|\alpha\rangle = \frac{\partial E_\alpha}{\partial\tau_k} \quad (3)$$

$$= 2 \sum_{P_k} V_k^{\alpha\alpha}(\boldsymbol{\tau}; P_k) \quad (4)$$

suggests the diagonal matrix element of the perturbation as the fundamental object. P_k represents the polyad, associated with the resonance \hat{V}_k , whose constancy is destroyed in the presence of other independent resonant perturbations. Consequently[16, 25] dominance of $V_k^{\alpha\alpha}(\boldsymbol{\tau}; P_k)$ at a single P_k implies a highly localized $|\alpha\rangle$ in the state space with P_k being an approximate quantum number. Quantum mechanically if $|V_k^{\alpha\alpha}|$ is large then it is expected that the perturbation \hat{V}_k plays a role in determining the nature of $|\alpha\rangle$. On the other hand a semiclassical analysis of the expectation value provides valuable information on the phase space nature of $|\alpha\rangle$. This can be seen by considering the quantity $\rho_k(E) \equiv \sum_\alpha V_k^{\alpha\alpha} \delta(E - E_\alpha)$ which is the expectation values of \hat{V}_k weighted by the density of states. Such quantities lend themselves to an elegant semiclassical interpretation in terms of the classical closed orbits in the phase space. This is hardly surprising given that the genesis of the Gutzwiller periodic orbit quantization[27] idea was from a semiclassical analysis of the quantum density of states $\rho = \sum_\alpha \delta(E - E_\alpha)$. As the method of semiclassical analysis of $\rho_k(E)$ is well established in the literature and our intention in this work is not to semiclassically evalu-

ate $V_k^{\alpha\alpha}$ we will highlight the salient features. In general ρ_k has a smooth and oscillating part with the smooth part being independent of the nature of the classical dynamics. The oscillating part is sensitive to the nature of the dynamics and can be written down in terms of a sum over the closed orbits in the phase space. If the phase space is chaotic then the closed orbits are the various periodic orbits whereas for a regular phase space the closed orbits are the rational tori. In either case it can be shown[26] that the oscillating part depends inversely on the determinant of the stability matrix M of the closed orbit and directly on the quantity

$$V_{kp} = \frac{1}{T_p} \int_0^{T_p} dt V_k(\boldsymbol{\theta}(t), \mathbf{I}(t)) \quad (5)$$

representing the average of the resonant term over one period T_p of the closed orbit.

We emphasise the dependence of ρ_k on the quantities M and V_{kp} for two reasons. Firstly, V_{kp} clearly underscores the important role played by the classical analog of \hat{V}_k . Further, performing a standard canonical transformation $(\mathbf{I}, \boldsymbol{\theta}) \rightarrow (J, \psi, \mathbf{K}, \boldsymbol{\chi})$ with (J, ψ) being the slow angle and action variables specific to the resonant term $\cos(\mathbf{m}_k \cdot \boldsymbol{\theta})$ we obtain

$$V_{kp} = \frac{1}{T_p} \int_0^{T_p} dt f_k(J, \mathbf{K}) \cos \psi \quad (6)$$

Now for a closed orbit in the phase space corresponding to $\mathbf{m}_k \cdot \boldsymbol{\theta} = 0$ the angles $\boldsymbol{\chi}$ are fast and can be averaged resulting in the actions $\mathbf{K}(t) \approx \mathbf{K}(0)$. The fixed points for the averaged system are then determined by $(J_p, \psi_p) = (0, 0)$ and correspond to the closed orbit in the full phase space. Within this averaged viewpoint $V_{kp} \approx \pm f_k(J_p, \mathbf{K})$ with the signs coming from $\psi_p = 0, \pm\pi$. Thus it is expected that a maximum in $|V_k^{\alpha\alpha}|$ comes from the localization of the eigenstate $|\alpha\rangle$ due to closed orbits associated with \hat{V}_k . Evidently states influenced by a particular closed orbit can be classified into a group and identified by patterns in the $V_k^{\alpha\alpha}$ ‘‘spectrum’’. In mixed phase space regimes, generic to molecular systems, periodic orbits with varied stabilities can exist and influence the dynamics. In the following sections we show the expectation values which are scaled to unit variance and zero centered. The scaling is performed to remove the dependence[22, 25] of $V_k^{\alpha\alpha} \propto P_k^{O_k/2}$ on the approximate polyad P_k arising from the localization of the eigenstate $|\alpha\rangle$ due to \hat{V}_k .

Secondly, bifurcations in the phase space are signalled by the vanishing[7] of the determinant $\det|(M - 1)|$. In general bifurcations imply birth of new orbits and/or death of old orbits. In the molecular context[9] such bifurcations manifest themselves as destruction of the old modes and creation of the new modes which influence the eigenstates. For instance a normal to local transition with varying energy arises due to bifurcations in the classical phase space. Thus it is natural to expect that

the $V_k^{\alpha\alpha}$ “spectrum” will exhibit the effects of the various bifurcations.

Recent work from our group has demonstrated the usefulness of the above method for understanding the highly excited states of a model system[25] and the DCO radical[16]. In this letter two molecules, CHBrClF and C_2H_2 , are chosen as further examples to illustrate the method. Specifically, the $N = 5$ polyad of CHBrClF and the $[16, 0]^{g+}$ bending polyad of C_2H_2 are investigated. In section II the highly excited states of CHBrClF are analyzed and compared to a recent work[13]. We find some discrepancy in the dynamical assignments provided earlier and by the level velocity method. In section III the pure bending states of C_2H_2 are investigated and it is shown that the level velocity approach is capable of identifying the new class of local bending and counter-rotation states. Comparing to a recent work[29] we show that the level velocity approach is successful in identifying important eigenstate sequences at such high levels of excitation. Section IV concludes.

II. DYNAMICAL NATURE OF CHBRCLF EIGENSTATES IN POLYAD $N = 5$

An effective Hamiltonian for CHBrClF was proposed by Beil *et al.* on the basis of their detailed study of the rovibrational spectra[28]. The CH overtone spectrum implicated multiple Fermi resonances involving the pure CH stretch (s) and the two (a, b) CH bending vibrations. The spectroscopic Hamiltonian has the form:

$$\hat{H} = \hat{H}_0 + k_{saa}\hat{V}_{saa} + k_{sbb}\hat{V}_{sbb} + k_{sab}\hat{V}_{sab} + \gamma\hat{V}_{aabb} \quad (7)$$

The zeroth-order anharmonic part is diagonal in the number (v_s, v_a, v_b) basis

$$H_0 = \sum_j^{sab} \nu_j v_j + \sum_j^{sab} \sum_k^{sab} x_{jk} v_j v_k \quad (8)$$

with the ν_j and x_{jk} being the harmonic frequencies and anharmonicities of the three modes respectively. The perturbations \hat{V} are off-diagonal in the (v_s, v_a, v_b) basis and represent resonant coupling of the modes. The first three perturbation terms in the Hamiltonian are Fermi resonances between the CH stretch and the various bend modes whereas the last perturbation is a Darling-Dennison resonance between the two bend modes. The structure of the effective Hamiltonian implies the existence of a constant of the motion $N = v_s + (v_a + v_b)/2$ called as the polyad number. For the various parameter values and form of the resonant operators we refer the reader to the earlier works[13, 28]. However, we note that the bending mode anharmonicities x_{aa}, x_{bb}, x_{ab} are small and the resonant coupling strengths are rather large. For instance, $x_{aa} \sim -6 \text{ cm}^{-1}$ and the stretching mode anharmonicity $x_{ss} \sim -65 \text{ cm}^{-1}$ whereas $k_{sbb} \sim 113$

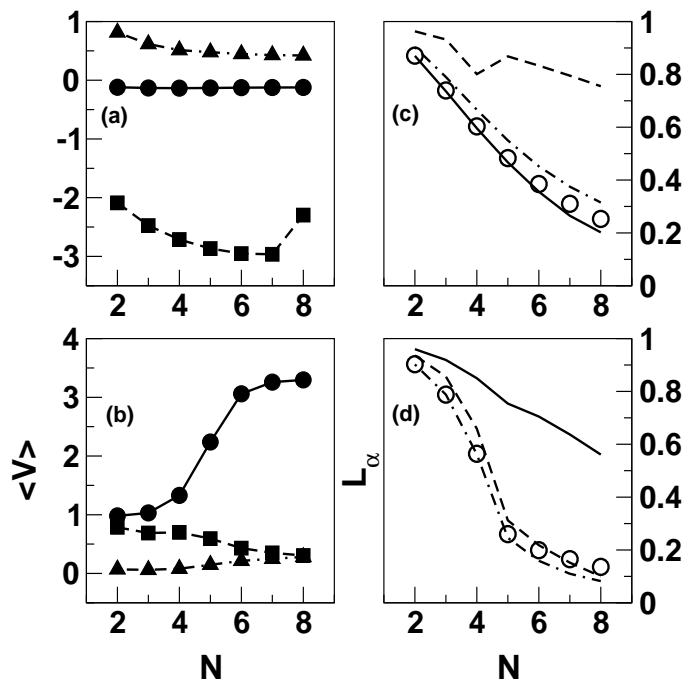


FIG. 1: Resonance expectation values as a function of the polyad $N = v_s + (v_a + v_b)/2$ for (a) lowest and (b) highest energy states in a polyad for CHBrClF. The circles, squares and triangles represent the expectation values of \hat{V}_{saa} , \hat{V}_{sbb} , and the \hat{V}_{aabb} respectively. The IPRs for the two sets of states are shown in (c) and (d). Open circles denote IPRs in the zeroth order basis and the solid line, dashed line, dash-dotted lines represent IPRs in the $H_0 + V_{saa}$, $H_0 + V_{sbb}$, $H_0 + V_{aabb}$ basis respectively.

cm^{-1} . Such large resonant strengths combined with reduced bend anharmonic constants imply that any analysis solely based on H_0 would be inadequate.

We also report the inverse participation ratios (IPR) of the eigenstates in various basis. The IPR L_α of an eigenstate $|\alpha\rangle$ in a basis $|b\rangle$ is given by $L_\alpha = \sum_b |\langle b|\alpha\rangle|^4$. L_α is a measure of the extent of delocalization of an eigenstate in a specific basis. A high L_α indicates localization in the state space whereas for a completely delocalized state $L_\alpha = 1/N_s$ with N_s being the total number of states.

In this work we focus on the $N_s = 36$ eigenstates belonging to the polyad $N = 5$ in the energy range of $[11361, 13947] \text{ cm}^{-1}$. In order to determine the possibility of bifurcations with varying N in Fig. 1a,b we show the relevant expectation values as a function of increasing N for the lowest and highest energy states respectively in a given polyad. The expectation values of \hat{V}_{sab} are relatively small and hence not shown in the figures. The IPRs in the zeroth order basis and various integrable single resonant basis are shown in Fig. 1c,d. For the lowest energy state it is clear that the sbb -Fermi resonance plays an important role. This is evident from the IPR information as well since the sbb single resonance basis values are fairly high for the range of N shown. On the other hand the highest energy states show the importance of

the *saa*-Fermi resonance. The sharp rise in the expectation value corresponding to V_{saa} between $N = 4$ and $N = 6$ indicates a change in the nature of the dynamics which is confirmed by studying the surface of sections. In both instances the dominance of a single $\langle V \rangle$ and the corresponding single resonance basis IPR establishes the states to be regular and highly localized.

In Fig. 2 the relevant $\langle V \rangle$ are shown for the eigenstates in $N = 5$. Note that a large $|V_k^{\alpha\alpha}|$ implies a localized state in the corresponding state space resonance zone and also in the phase space about a closed orbit. The nature of the closed orbit *i.e.*, stable or unstable is inferred from the sign of $V_k^{\alpha\alpha}$. A look at the partial expectation values $V_k^{\alpha\alpha}(P_k)$ will reveal a single dominant contribution leading to the assignment (N, P_k, ν) with ν denoting an excitation index for states with the same P_k . We will not give a list of assignments for the states in $N = 5$ but rather focus on certain eigenstate sequences in order to compare to a recent work[12]. At first glance it is apparent that the *sbb* resonance is influencing the lower end of the polyad whereas the *saa* resonance is important for the higher energy states. Note, however, that with increasing energy the *saa* rapidly gains significance with concomitant decrease in the *sbb* influence. From Fig. 2 it is seen that around 12020 cm^{-1} $\langle V_{saa} \rangle \approx \langle V_{sbb} \rangle$ and the sequence splits into two branches. This indicates a change in the underlying phase space and thus localization nature of the eigenstates on the two branches should be different. This is supported by examining the phase space and the alternating assignments provided in a recent work[13]. At the same time towards the middle of the polyad the Darling-Dennison resonance is playing a key role in organizing the eigenstates. We plot the $\langle V \rangle$ versus the energy eigenvalues E_α since this immediately reveals the states that are possibly involved in avoided crossings. In Fig. 2 certain sequences have been shown and labeled according to a classification done recently. In this classification[13] *B* represent nonresonant states, and *C* represent states influenced by the Darling-Dennison resonance. From the expectation values, however, it is not apparent that the first few states are nonresonant. Indeed our analysis suggests some of these states, for instance the first three states, are influenced by the *sbb* Fermi resonance. That this is indeed the case has been confirmed by the method of local frequency analysis which shows extensive *sbb* locking. In addition the corresponding IPRs in the single *sbb* resonance basis are very high suggesting strong influence by the resonance. Thus state number one is assigned as $(N = 5, P_{sbb} \equiv 2v_s + v_b = 10, v_a = 0)$ rather than the earlier assignment of $(N = 5, v_a = 0, v_b = 10)$.

The earlier assignment[13] of Darling-Dennison states essentially agrees with our results. Certain strongly localized sequence of *C* states is immediately revealed by the expectation values as evident from Fig. 2. It is expected that such states are localized about the stable periodic orbit associated with the \hat{V}_{aabb} which has been confirmed by computing the Husimi distribution functions. Our assignment for the state denoted C_{50} is

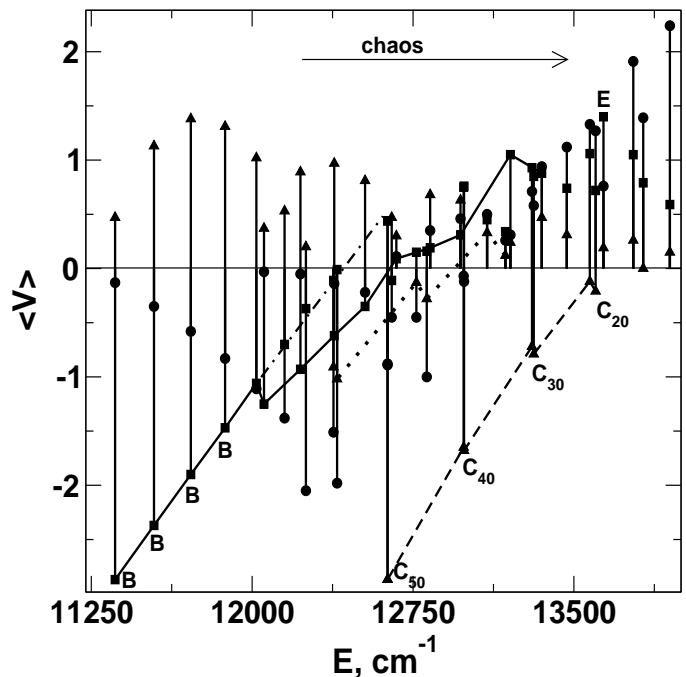


FIG. 2: Resonance expectation values for the states belonging to $N = 5$ for CHBrClF. The horizontal zero-line is shown for ease of visualization. The symbols used are identical to the ones used in Fig. 1. The approximate energy at which large scale chaos sets in the phase space is indicated. Some of the eigenstate sequences are shown and labeled as in an earlier work[13]. Note the particularly large values for certain states indicating localization in state space and phase space. Also note that around 12020 cm^{-1} the expectation values $\langle V_{saa} \rangle \approx \langle V_{sbb} \rangle$ and the splitting of the 'B' sequence into two shown by dash-dotted line. Further details are provided in the text.

$(N = 5, P_{aabb} \equiv v_a + v_b = 10, v_s = 0)$ and clearly the approximate polyad P_{aabb} can be identified with the longitudinal quantum number n_l introduced in the earlier work[13]. Indeed the maximum magnitude of the expectation $V_{aabb}^{\alpha\alpha}$ can be estimated as $P_{aabb}^2/4$ and state C_{50} shows close agreement with this classical estimate. The so called transverse quantum number n_t is associated with the degree of excitation ν for a given P_{aabb} . In the $n_t = 0$ sequence it is clear from the figure that with increasing energy other resonances are coming into effect. The state labeled C_{20} , in particular, is strongly influenced by both the *saa* and the *sbb* Fermi resonances and hence it is inappropriate to classify them as Darling-Dennison states. The sequence corresponding to $n_t = 1$ is strongly perturbed by the *saa* Fermi resonance.

Finally state number 16 and 30 have been classified in the previous work as "chaotic" states (class *D*) exhibiting a mixture of class *B* and class *C* states. The present analysis supports the above classification for state 16, which incidentally has the lowest IPR among all the states, but clearly Fig. 2 suggests state 30 to be different. The large expectation values of *saa* with smaller *sbb* expectation

values indicates this state to be influenced by the *saa* and *sbb* resonances. This state can be nominally assigned as ($N = 5, P_{saa} \equiv 2v_s + v_a = 8, v_b = 2$). Similarly state number 33 was classified as $E(D)$ suggesting dominant *saa* character. However state space, expectation values (cf. Fig. 2) and the various IPRs (integrable single *sbb* resonance basis IPR is about 0.7) point to a state with *sbb* character.

III. NATURE OF THE HIGHLY EXCITED BEND STATES IN C_2H_2

The pure bending dynamics of acetylene at about 10000 cm^{-1} above ground state is known to be quite complicated due to the strong interaction between the trans and the cis bending normal modes[11]. However recent work by Jung, Taylor and Jacobson revealed that the highly excited bending eigenstates were assignable despite strong chaos in the system[29]. The key to their dynamical assignments was the fact that a few periodic orbits were organizing the dynamics at such high energies and hence influencing the structure of the eigenstates. Many sequences of eigenstates exhibiting similar localization patterns about the periodic orbits were identified leading to the unzipping of the spectrum. The purpose of this section is to show that parametric variations can immediately reveal the existence of such progressions without the need for the visualization of the phase space and/or the eigenstates.

The effective Hamiltonian appropriate for the study of the bend only dynamics up to 15000 cm^{-1} with an accuracy of 1.5 cm^{-1} has the form[30] $\hat{H} = \hat{H}^{\text{lin}} + \hat{H}^{\text{anh}} + \hat{H}^{\text{int}}$. The harmonic part $\hat{H}^{\text{lin}} = \omega_4 \hat{v}_4 + \omega_5 \hat{v}_5$ and the anharmonic part is given by

$$\hat{H}^{\text{anh}} = \sum_{j,k=4,5} (x_{jk} v_j v_k + g_{jk} l_j l_k) + \sum_{jkl=4,5} y_{jkl} v_j v_k v_l \quad (9)$$

with v_4 and v_5 representing the number of quanta in the trans and cis normal modes respectively. The degenerate bends further require the vibrational angular momenta l_4 and l_5 . Thus the zeroth order states, eigenstates of $\hat{H}^{\text{lin}} + \hat{H}^{\text{anh}}$, are denoted by $|v_4^{l_4} v_5^{l_5}\rangle$. However $\hat{H}^{\text{int}} = \hat{V}_{DDI} + \hat{V}_{DDII} + \hat{V}_{ll}$ couples the zeroth order states via the off-diagonal anharmonic resonances. \hat{V}_{DDI} is a Darling-Dennison resonance leading to exchange of quanta between the two modes at constant l_4 and l_5 whereas \hat{V}_{ll} is a vibrational l -resonance which leads to exchange of vibrational angular momentum only between the two modes. \hat{V}_{DDII} results in both exchange of quanta and vibrational angular momentum between the two modes. For the fitted parameter values and form of the perturbation operators we refer the reader to the previous works[29, 30]. Due to the nature of the resonant couplings there are two conserved quantum numbers or polyads denoted by $N_b = v_4 + v_5$ and $l = l_4 + l_5$. In addition eigenstates respect certain symmetries and hence

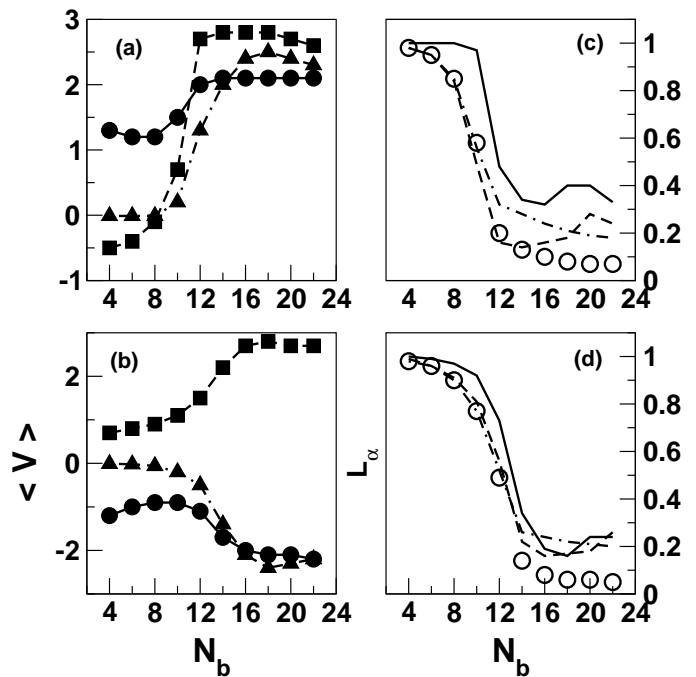


FIG. 3: Expectation values as a function of the bend polyad $N_b = v_4 + v_5, l = 0$ for (a) lowest and (b) highest energy states in a polyad for C_2H_2 . Circles, squares and triangles denote the expectation values $\langle V_{DDI} \rangle$, $\langle V_{DDII} \rangle$, and $\langle V_{ll} \rangle$ respectively. Note the sharp change around $N_b = 12$ and $N_b = 14$ for the lowest and highest states respectively. The IPRs in various basis for the two states are shown in (c) and (d) as a function of N_b . IPR in the zeroth order basis are denoted by open circles and in the various single resonance basis by lines ($H_0 + V_{DDI}$ by solid line, $H_0 + V_{DDII}$ by dashed line, and $H_0 + V_{ll}$ by dot-dashed line).

labelled by \pm (parity under say $l_4 \rightarrow -l_4$) and g/u (v_5 even/odd). There are a total of 81 states for the polyad $N_b = 16$ spanning an energy range of $[10239, 11255]\text{ cm}^{-1}$. Although it is possible to analyze all of the eigenstates, in this letter we focus on the subset of eigenstates with $N_b = 16$ and $l = 0$ and symmetry class $g+ i.e.$, states belonging to $[16, 0]^{g+}$. Note that there are a total of 25 states in $[16, 0]^{g+}$. As in the previous section we will be interested in the expectation values (three of them for acetylene) $V_j^{\alpha\alpha}$.

To begin with we consider, in analogy with the previous section, the possibility of various bifurcations occurring in C_2H_2 with varying polyad N_b . Earlier studies[11] have revealed that the lowest (trans bend) and highest (cis bend) energy eigenstates in a given polyad undergo a sharp change in character with increasing N_b . More precisely, around $N_b = 12$ the lowest state is not the usual trans bend and becomes a local bend whilst around $N_b = 14$ the highest state changes character from a cis bend to the so called counter-rotator mode. Such changes are characteristic of bifurcations which lead to new types of modes (dynamics) and we expect the expectation values to be sensitive indicators of these changes. In order to

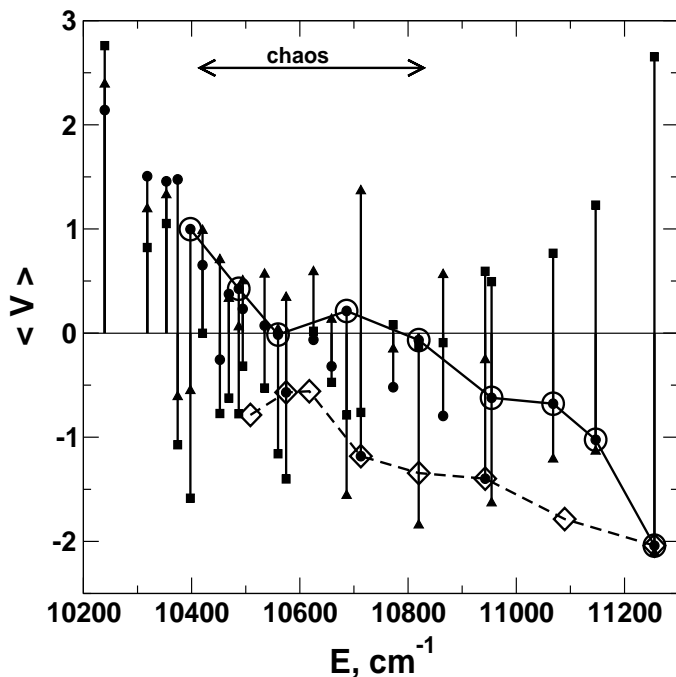


FIG. 4: Expectation values for the states belonging to the $[16, 0]^{g+}$ polyad of C_2H_2 . Symbols used are identical to those in Fig. 3. Open Diamonds mark a sequence of eigenstates representing the family I and open circles indicate the sequence of eigenstates representing the family II as in an earlier work[29]. The lines are drawn as a guide to the eye. Note some of the family I states are $|u\rangle^+$ states shown in this plot for clarity. The approximate energy region over which considerable chaos exists in the classical dynamics is also indicated. See text for discussions.

show this in Fig. 3a,b we show the $\langle V \rangle$ for the lowest and the highest energy states as a function of N_b . As expected the $\langle V \rangle$ very clearly indicate the sharp nature of the bifurcations in agreement with the previous observations. In Fig. 3c,d we have also shown the IPRs of the states in various basis for comparison. Note that the IPRs also indicate the transition. However, the various IPRs in the post transition regime take on very small values and by definition this indicates that many zeroth order normal modes are contributing to the eigenstates and thus suggesting highly mixed states. Contrast this with the fact that all of the expectations are very large suggesting highly localized states. The resolution to these apparently conflicting observations lies in realizing that new types of dynamics *i.e.*, periodic orbits created due to the bifurcations are influencing the eigenstates and the zeroth order normal modes are a poor basis to understand the new modes. It is important to note that IPR in any single resonance (dressed) basis is also an insufficient indicator of the new modes. The expectation values on the other hand are quite sensitive and the nature of the new modes can be deciphered with further analysis[12].

We now turn to an analysis of the states in $[16, 0]^{g+}$. In Fig. 4 the expectation values are shown for all the states.

Based on previous observations it is easy to identify the local bend and the counter rotating states at the energetic minimum and maximum of the polyad. The appearance of rather complicated behaviour in the middle of the polyad is related to the occurrence of bifurcations with varying energy[29]. Further understanding can be gained by analyzing the reduced classical Hamiltonian[29]:

$$\begin{aligned}
 H(\mathbf{J}, \psi; \mathbf{K}) = & H_0(\mathbf{J}; \mathbf{K}) + 2s_{45}f_a(\mathbf{J}; \mathbf{K}) \cos \psi_a \\
 & + 2r_{45}f_b(\mathbf{J}; \mathbf{K}) \cos \psi_b \\
 & + 2t_{45}[f_-(\mathbf{J}; \mathbf{K}) \cos(\psi_a - \psi_b) + f_+(\mathbf{J}; \mathbf{K}) \cos(\psi_a + \psi_b)]
 \end{aligned} \tag{10}$$

where $\mathbf{J} = (J_a, J_b) \equiv ((v_4 - v_5)/4, (l_4 - l_5)/4)$, $\mathbf{K} = (K_a, K_b) \equiv ((N_b + 2)/4, l/4)$, and $t_{45} = (r_{45} + 2g_{45})/4$. The angles ψ_a and ψ_b correspond to the DDI and the vibrational- l resonances respectively. The angle combinations $\psi_a \pm \psi_b$ correspond to the DDII resonance. The fixed points of the above Hamiltonian *i.e.*, $(\dot{\mathbf{J}}, \dot{\psi}) = (\mathbf{0}, \mathbf{0})$ represent the periodic orbits of the full system. It is easy to see that in the angle space the fixed points are $\psi_{a,b} = 0, \pm\pi$. From our discussions we expect the functions f_a, f_b , and (f_-, f_+) at the fixed points to indicate the 'dynamical' nature of a specific eigenstate. In particular, the signs of the various expectations provide information on the nature of eigenstate localization in the (ψ_a, ψ_b) space. It is easy to see that four possible sign combinations $+++$, $+--$, $---$, and $-+-$ are possible corresponding to the localization about $(0, 0)$, $(0, \pi)$, (π, π) , and $(\pi, 0)$ respectively. At this stage we emphasize that highly localized eigenstates imply a specific sign combination and large magnitude expectation(s). Thus, for instance, from Fig. 4 we anticipate that the states $|g\rangle_1^+$, $|g\rangle_4^+$, $|g\rangle_{25}^+$, and $|g\rangle_{17}^+$ are highly localized states about $(0, 0)$, $(0, \pi)$, (π, π) , and $(\pi, 0)$ respectively. These states exhibit localization in phase space as well. We find a total of 18 states that belong to one of the four sign combinations. On the other hand there are states that do not belong to one of the above four classes. For example $|g\rangle_{14}^+$ has the sign combination $-++$ and small expectation values. This suggests a fairly delocalized state which is hard to assign dynamically. Similarly state $|g\rangle_{19}^+$ comes with the sign combination $---$ but Fig. 4 clearly implies a localized state influenced by the vibrational- l resonance alone. Interestingly such states are precisely the ones that were multiply assigned in the previous study[29].

Jung *et al.* have used the semiclassical representation of the eigenstates[31] in the (ψ_a, ψ_b) space to provide a sequence of similarly localized states[29]. Two main families, I and II, were identified based on the excitation along specific periodic orbits. In Fig. 4 we show two such sequences, one from each family, as seen from the perspective of the expectation values. It is apparent that the family I is more robust than the family II sequence. This is directly related to the fact that the periodic orbit underlying family I undergoes far fewer bifurcations as compared to the periodic orbit corresponding to family II. However even in the family I sequence two states $|u\rangle_{12}^+$

and $|g\rangle_{13}^+$ are significantly perturbed. There can be many sources for such perturbations and in this case it happens to be an avoided crossing. Nevertheless from Fig. 4 it is clear that the state $|g\rangle_{13}^+$ is localized mainly due to the DDII resonance.

IV. CONCLUSIONS

In this letter we have demonstrated the utility of eigenstate expectation values of resonant perturbations in understanding the nature of highly excited vibrational states. A particularly large expectation value implies that the associated eigenstate is localized and influenced by a closed orbit in the classical phase space. Existence of localized states and their sequences can be ascertained by inspecting the expectation values (magnitude and sign) and the IPRs irrespective of whether the classical phase space is (near)-integrable, mixed or chaotic. In case of complete chaos, from random matrix theory arguments, a typical expectation value is expected[32] to be $1/\sqrt{N_s}$. The examples studied here are quite far from such a limit. Combined with the relative signs of the expectation values it is possible to identify specific eigenstate sequences. Sensitivity of the expectation values to the bifurcations provides information on the birth of new types of modes and the resulting perturbations on the eigenstate sequences. Currently it is not possible to identify the type of bifurcation that occurs and this aspect needs further study. It is important to note that we are not advocating the use of periodic orbits to compute the expectation values which is a difficult task. Instead we are emphasizing the manifestation and utility of such classical structures in a fundamental quantum object *i.e.*, an

expectation value. Similar philosophy has been adopted in the 'vibrogram' or (E, τ) approaches to study resonant systems[33, 34] This classical-quantum correspondence aspect of the expectation values can be easily applied to multidimensional coupled systems without the need for determining/visualization of phase space, periodic orbits or eigenstates. Indeed preliminary work on a coupled 4-mode effective Hamiltonian suggests that such an approach is useful.

Finally we note that Jacobson and Field have recently[35] studied expectation values of resonance operators for a nonstationary state. Choosing the nonstationary state to be a zeroth order bright state $|\mathbf{v}\rangle$ it was shown that the time-dependent expectations $\langle \mathbf{v}(t) | \widehat{V}_k | \mathbf{v}(t) \rangle$ indicate the resonances important for dynamics over a particular time interval. Relation to the present work is realized by the fact that

$$\lim_{T \rightarrow \infty} \frac{1}{T} \int_0^T \langle \mathbf{v}(t) | \widehat{V}_k | \mathbf{v}(t) \rangle = \sum_{\alpha} |\langle \mathbf{v} | \alpha \rangle|^2 V_k^{\alpha\alpha} \quad (11)$$

Thus the time-dependent expectations are, in the infinite time limit, nothing but intensity weighted eigenstate expectation values. Such an object, the intensity-velocity correlator, has been recently introduced and studied in great detail[36].

V. ACKNOWLEDGEMENTS

This work is supported by funds from the Department of Science and Technology, India.

-
- [1] R. Marquardt and M. Quack, *Encyclopedia of Chemical Physics and Physical Chemistry*, Vol.I, Ed. J. H. Moore, IOP, Bristol, 2001.
- [2] T. Uzer, Phys. Rep. **199**, 73 (1991).
- [3] D. J. Nesbitt, R. W. Field, J. Phys. Chem. **100**, 12735 (1996).
- [4] M. Gruebele, Adv. Chem. Phys. **114**, 193 (2000).
- [5] A. B. McCoy, E. L. Sibert III in *Dynamics of Molecules and Chemical reactions*, Ed. R. E. Wyatt and J. Z. H. Zhang, Dekker, NY 1996.
- [6] M. Joyeux, D. Sugny, Can. J. Phys. **80**, 1459 (2002).
- [7] A. J. Lichtenberg, M. A. Lieberman, *Regular and Stochastic Motion*, Springer, NY 1983.
- [8] See, M. V. Kuzmin, A. A. Stuchebrukhov in *Laser Spectroscopy of Highly vibrationally Excited Molecules*, Ed. V. S. Letokhov, pp. 178, Adam Hilger, Bristol, 1989.
- [9] M. E. Kellman, Adv. Chem. Phys. **101**, 590 (1997).
- [10] M. Joyeux, S. C. Farantos, R. Schinke, J. Phys. Chem. A, **106**, 5407 (2002).
- [11] M. P. Jacobson, R. W. Field, J. Phys. Chem. A **104**, 3073 (2000).
- [12] M. P. Jacobson, C. Jung, H. S. Taylor, R. W. Field, J. Chem. Phys. **111**, 600 (1999).
- [13] C. Jung, E. Ziemniak, H. S. Taylor, J. Chem. Phys. **115**, 2499 (2001).
- [14] H. Ishikawa, R. W. Field, S. C. Farantos, M. Joyeux, J. Koput, C. Beck, R. Schinke, Annu. Rev. Phys. Chem. **50**, 443 (1999).
- [15] S. Keshavamurthy, G. S. Ezra, J. Chem. Phys. **107**, 156 (1997).
- [16] A. Semparathi, S. Keshavamurthy, Phys. Chem. Chem. Phys. **5**, 5051 (2003).
- [17] However, see C. Jung, C. Mejia-Monasterio, H. S. Taylor, J. Chem. Phys. **120**, 4194 (2004).
- [18] R. Ramaswamy, R. A. Marcus, J. Chem. Phys. **74**, 1379 (1981).
- [19] J. P. Rose, M. E. Kellman, J. Chem. Phys. **104**, 10471 (2000).
- [20] P. Wang, G. Wu, Chem. Phys. Lett. **371**, 238 (2003).
- [21] B. Ramachandran, K. G. Kay, J. Chem. Phys. **99**, 3659 (1993).
- [22] S. Keshavamurthy, J. Phys. Chem. A **105**, 2668 (2001).
- [23] M. S. Child, J. Mol. Spec. **210**, 157 (2001).
- [24] Y. Weissman, J. Jortner, J. Chem. Phys. **77**, 1486 (1982).

- [25] A. Semparithi, V. Charulatha, S. Keshavamurthy, J. Chem. Phys. **118**, 1146 (2003).
- [26] B. Eckhardt, S. Fishman, K. Müller, D. Wintgen, Phys. Rev. A **45**, 3531 (1992).
- [27] M. C. Gutzwiller, *Chaos in Classical and Quantum Mechanics*, Springer, NY 1990.
- [28] A. Beil, D. Luckhaus, M. Quack, Ber. Bunsenges. Phys. Chem. **100**, 1853 (1996).
- [29] C. Jung, H. S. Taylor, M. P. Jacobson, J. Phys. Chem. A **105**, 681 (2001).
- [30] M. P. Jacobson, J. P. O'Brien, R. J. Silbey, R. W. Field, J. Chem. Phys. **109**, 121 (1998).
- [31] E. L. Sibert, A. B. McCoy, J. Chem. Phys. **105**, 469 (1996).
- [32] F. Haake, *Quantum Signatures of Chaos*, 2nd edition, Springer, Berlin, 2001. Considerable work has been done towards understanding the parametric variation in a variety of systems and chapter 6 of this book provides an introduction to this vast field.
- [33] G. S. Ezra, Adv. Class. Traj. Meth. **3**, 35 (1998) and references therein.
- [34] P. Gaspard, I. Burghardt, Adv. Chem. Phys. **101**, 491 (1997).
- [35] M. P. Jacobson, R. W. Field, Chem. Phys. Lett. **320**, 553 (2000).
- [36] See S. Keshavamurthy, N. R. Cerruti, S. Tomsovic, J. Chem. Phys. **117**, 4168 (2002) and references therein.